

Purification of endogenous Rpd3S complex

The Rpd3S complex was purified from a yeast strain containing a 2xFlag tag at the C terminus of Rco1 subunit. The tagged yeast strain was grown in 10 L YPD medium overnight at 30°C. Cells were collected by centrifugation and resuspended in lysis buffer (50 mM Tris pH 7.6, 300 mM ammonium sulfate, 1 mM EDTA, 10 uM ZnCl₂, 10% glycerol and protease inhibitor cocktail). The cell suspension was frozen in liquid nitrogen and milled to powder using a cryogenic grinder (Spex sample prep 6875). The powder was thawed at 4°C and centrifuged at 16,000 g for 30 min to remove cell debris. The supernatant was centrifuged in a Beckman Optima XE-90 ultracentrifuge with a Beckman Type 45 Ti rotor at 40,000 rpm for 2 hours at 4°C. The clarified supernatant was selectively precipitated in 30%-55% ammonium sulfate and resuspended in binding buffer (25 mM Tris pH 7.6, 100 mM ammonium sulfate, 1 mM EDTA, 10 uM ZnCl₂, 10% glycerol and protease inhibitor cocktail). For the affinity purification, 0.5 ml Anti-FLAG M2 affinity beads (Sigma) were incubated with the supernatant at 4°C for 2 hours. The beads were next washed and resuspended in 1ml elution buffer (25 mM HEPES pH 7.6, 100 mM ammonium sulfate, 1 mM EDTA, 10% glycerol). Protein elution using 10 mM 3xFLAG peptide (Sigma) was performed at 4°C for 3 hours with gentle shaking. The eluate was concentrated and loaded onto a Superose 6 10/300 GL column (GE Healthcare Life Sciences) for further purification with SEC buffer (25 mM HEPES pH 7.6, 100 mM NaCl, 1 mM EDTA, 10% glycerol). The peak fractions containing the Rpd3S complex were combined and aliquoted, flash frozen in liquid nitrogen and stored at -80°C. For each purification step, the Rpd3S complex was monitored with purity and structural integrity by SDS-PAGE and EM examination.

Preparation of histone H3 modified with Kc36me3

To generate the histone H3 with Kc36 trimethylation, mutations (K36C, C110A) were introduced into the H3 sequence by site-directed mutagenesis. The cysteine was alkylated to create *N*-methylated aminoethylcysteine residues, an analog of methyl-lysine, as previously described¹. Briefly, 10 mg freeze-dried histones were dissolved in alkylation buffer (1 M HEPES pH 7.8, 4 M guanadinium chloride, 10 mM D/L-methionine) and reduced with DTT at 37°C for 1 hour. 100 mg (2-bromoethyl) trimethylammonium bromide (Sigma) was added and incubated at 50°C for 5 hours with occasional mixing.

The reactions were quenched with 5 mM β -mercaptoethanol and dialyzed to 3 mM β -mercaptoethanol/H₂O. The modified histone H3 was aliquoted, lyophilized, and stored at -80°C. The appropriate trimethylation was confirmed by western blotting using H3K36me3 antibody (Abcam: ab9050).

Preparation of mononucleosome with 216 bp DNA

Xenopus laevis histones H2A, H2B, H3-K36C/C100A and H4 were expressed respectively in *E. coli* BL21(DE3) as previously described^{2,3} with modifications. The histones were purified from the inclusion body using SP sepharose resin under denaturing condition, further purified using a YMC-Pack PROTEIN-RP column with HPLC (Waters: 2535q) and lyophilized. To prepare the octamer, histones H2A, H2B, H3-K36C/C100A and H4 were mixed in an equimolar ratio and dialyzed against the refolding buffer (10 mM Tris pH 7.5, 2 M NaCl, 1 mM EDTA, 5 mM β -mercaptoethanol). The octamer was purified by loading the mixture onto a Superdex 200 increase 10/300 GL column (GE Healthcare Life Sciences) with refolding buffer.

The 216 bp DNA fragment containing a linker DNA and a nucleosome positioning sequence (Widom 601)⁴ was generated by PCR. The PCR product was further purified by ion-exchange chromatography (Mono Q 5/50 GL, GE Healthcare Life Sciences) followed by isopropanol precipitation. The precipitated DNA pellet was dissolved in water, aliquoted, and stored at -20°C.

The sequence of 216 bp DNA with Widom 601 DNA underlined is as follows:

5'-

ACCATCGTCAGTATTGACTGCAGACCTGAAGCTTGATATCGAATTCGCGTGTC
GCCCTTACTGGCCGCCCTGGAGAATCCCGGTGCCGAGGCCGCTCAATTGGTC
GTAGACAGCTCTAGCACCGCTTAAACGCACGTACGCGCTGTCCCCCGCGTTTT
AACCGCCAAGGGGATTACTCCCTAGTCTCCAGGCACGTGTCAGATATATACA
TCCTGT-3'

Mononucleosome reconstitution was performed according to previously published protocols⁵ by salt-dialysis method, and purified by non-denaturing electrophoresis using a Prep Cell apparatus (Bio-Rad). The resulting nucleosome with H3Kc36me3 was concentrated to approximately 1 mg/ml and stored on ice until used.

Electrophoretic mobility shift assay

The Rpd3S-nucleosome complex was detected by electrophoresis on a 6% Native-PAGE gel in 0.2× TBE buffer at a constant voltage of 100 V for 1 hour. The gel was incubated for 10 min in TS-GelRed (Tsingke Biotechnology) containing NaCl buffer and visualized using an Imaging System (Tanon-2500).

HDAC activity assay

To measure the histone deacetylation activity of purified Rpd3S complex, the reaction was performed, as previously described⁶, in a buffer containing 25 mM Tris, 100 mM NaCl, 2 mM ZnCl₂, 1% glycerol, 100 μM fluorogenic substrate Boc-Lys(Ac)-AMC, pH 7.5. Reactions were initiated by adding 42 nM Rpd3S with and without 1 μM TSA and kept at room temperature for 1 hour. The reaction was stopped by the addition of 5 mg/ml trypsin and maintained for 1 hour at 37°C. The fluorescence intensities were measured with excitation at 350 nm and emission at 440 nm, using a multiscan spectrum (SpectraMax iD5). For the HDAC assay in the presence of 100 μM nucleosome, Rpd3S and 28 nM nucleosome were premixed and incubated on ice for 1 hour. Subsequent processes were performed as described above. The reaction was performed in triplicate, and the SD of the raw data is reported.

Cryo-EM sample preparation of Rpd3S-nucleosome complex

The Rpd3S was incubated with excess H3Kc36me3-modified nucleosome for 1 hour on ice. Excess nucleosome was removed by a Superose 6 10/300 GL column equilibrated in EM buffer (25 mM HEPES pH 7.6, 100 mM NaCl, 1 mM EDTA, 1 mM DTT, 2% glycerol). The fractions corresponding to Rpd3S-nucleosome complex were assessed by 6% Native-PAGE and SDS-PAGE, then collected and concentrated for cryo-EM grid preparation.

Cryo-EM grid preparation and data collection

For the Rpd3S complex, purified protein was diluted to approximately 50 μg/ml with the buffer (25 mM HEPES pH 7.6, 100 mM NaCl, 1 mM EDTA, 10% glycerol) and 3 μl of aliquots were applied onto freshly glow-discharged lacey carbon grids coated with a second layer of 3nm thick carbon film (TED PELLA). Samples were incubated on grids

for 20 s, blotted for 3.5 s and plunged frozen in liquid ethane. Cryo-EM grids were prepared with an EMGP2 (Leica company) set to 8°C and 95% humidity. The data was acquired on a Titan Krios electron microscope (FEI) at 300 keV equipped with a K2 summit direct electron detector (Gatan). A total of 4,724 movies were automatically recorded using SerialEM software at a nominal magnification of 18,000x, yielding a pixel size of 1.35 Å in counting mode, with defocus values ranging from -2.5 to -3.5 µm. The data was recorded with a total dose of 59 electrons per Å², recording 36 frames. For the Rpd3S-nucleosome complex, aliquots of 3 µl concentrated sample were loaded onto glow-discharged Quantifoil R2/1 Au 400 grids. After incubation for 20 s, the grids were blotted for 4 s and plunged frozen in liquid ethane. Grids were transferred to a Titan Krios transmission electron microscope (Thermo fisher) operating at 300 kV equipped with a Gatan Gif Quantum energy filter. Cryo-EM data was collected with EPU software through a Gatan K3 direct electron detector in counting mode at 81,000 x nominal magnification, resulting in a physical pixel size corresponding to 1.07 Å, with a defocus range of -1.8 to -2.8 µm. Exposure of 3.8 s was dose-fractionated into 32 moves frames, leading to a total accumulated dose of 53 electrons per Å² on the specimen. A total of 2,818 movies were saved as unprocessed Tiff files for analysis.

Image processing

The Rpd3S dataset:

Individual movie frames were aligned using MotionCor2⁷. CTF parameters were estimated using CtfFind4⁸. Particles were picked in Gautomatch (by K.Z., under development) using 2D averages obtained from negative staining data. Subsequent image processing was carried out in RELION-4.0-beta-2⁹ and cryoSPARC v3.3.2¹⁰. A total of 876,212 particles were extracted by four-times downscaling resulting in the pixel size of 5.4 with a box size of 84 x 84 pixels. Multiple rounds ab-initio reconstruction and heterogeneous refinement were run to get the best particles. The unbinned 73,857 particles were re-extracted and divided into three classes using heterogeneous refinement in cryoSPARC. Then the particles (24,648 particles; 25,950 particles; 23,259 particles) of these three conformations were reconstructed using non-uniform refinement, respectively. The final models were refined to an overall resolution of 9.84 Å, 8.68 Å and 8.82 Å.

1
2 The Rpd3S-nucleosome dataset:

3 The movies were imported into RELION-4.0-beta-2, and the whole-frame motion
4 correction was carried out by the RELION's own implementation with dose weighting.
5 Contrast transfer function (CTF) parameters were estimated using CTFFIND4.
6 Subsequently micrographs were rejected with extreme defocus values, too much
7 contamination or aggregation. Two particle subsets were initially picked using the
8 Gautomatch with the templates of Rpd3S and nucleosome, respectively, from the
9 remaining good 2,635 micrographs. The two subsets were extracted by four-times
10 downscaling resulting in the pixel size of 4.28 with a box size of 84 x 84 pixels, and
11 combined. The particles within the minimum inter-particle distance 30 Å were removed
12 leaving only one. Multiple rounds of reference-free 2D classification were run to remove
13 bad particles, and the following processes were performed using cryoSPARC v3.3.2.
14 After Ab-Initio reconstruction and heterogeneous refinement, a set of 130,804 particles
15 was re-extracted with the pixel size of 1.07. Further 3D classification was performed to
16 get homogeneous nucleosome-bound particles. The model was refined to an overall
17 resolution of 4.06 Å with 68,446 particles. To further improve the final resolution, a
18 series of 2D projections of the 4.06 Å map were used as template to re-pick particles
19 using Gautomatch. Subsequent processes were similarly performed as described above. A
20 final set of 107,252 Rpd3S-nucleosome complex particles was selected to perform a final
21 3D refinement, leading to a map with resolution at 3.72 Å. The same particles were
22 further used for particle subtraction, the Rpd3S core complex and nucleosome-Eaf3
23 complex, and further local refinement was carried out to obtain 3.37 Å and 3.58 Å maps.
24 The resolution values reported for all reconstructions were based on the gold-standard
25 Fourier shell correlation (FSC) 0.143 criterion.

26 27 **Model building and refinement**

28 A nucleosome structure (PDB 6S01) ¹¹ and the available structures of Rpd3S from
29 AlphaFold protein structure database ^{12,13} were fitted into the refined 3D reconstruction
30 map using UCSF Chimera ¹⁴ and then manually rebuilt in Coot ¹⁵. The remainder of the
31 molecules, including Rco1 N-ter, Rpd3 C-ter and linker DNA, were manually built based
32 on high-resolution maps in Coot. The model was subject to real-space refinement in

Phenix 1.18¹⁶. Structural analysis was performed in Coot, and figures were prepared using UCSF Chimera and ChimeraX¹⁷.

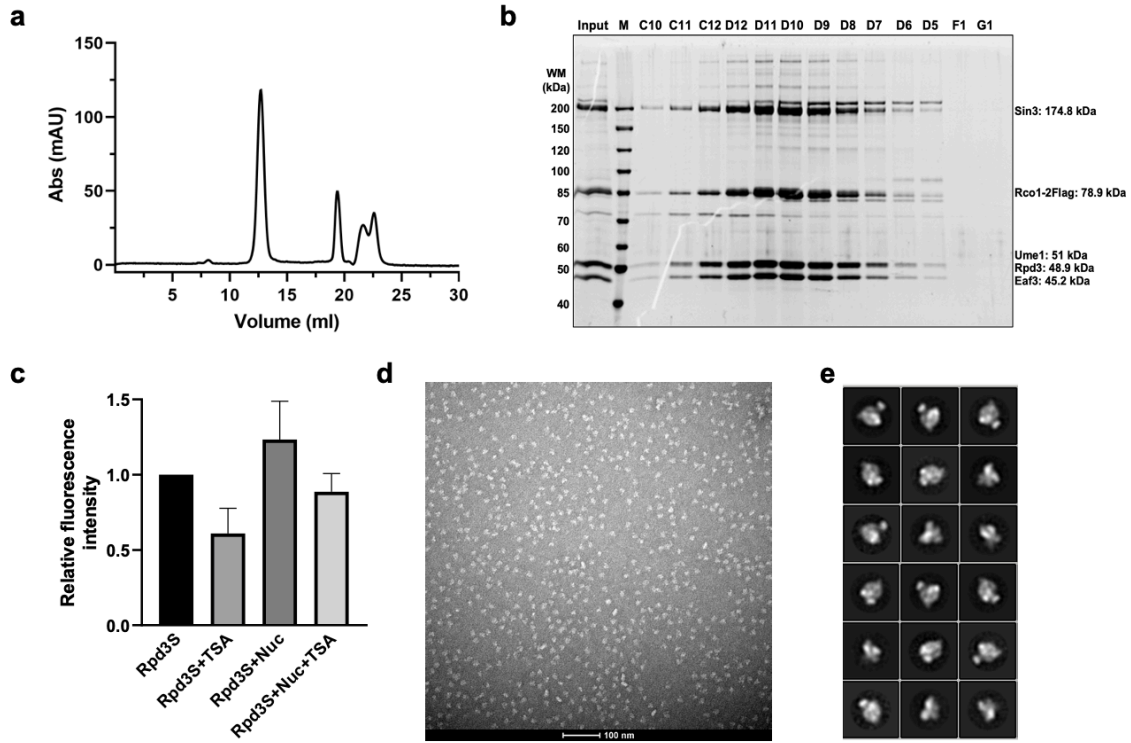
Reference:

- 1 Simon, M. D. *et al.* The site-specific installation of methyl-lysine analogs into recombinant histones. *Cell* **128**, 1003-1012 (2007).
<https://doi.org:10.1016/j.cell.2006.12.041>
- 2 Zhou, B. R. *et al.* Atomic resolution cryo-EM structure of a native-like CENP-A nucleosome aided by an antibody fragment. *Nat Commun* **10**, 2301 (2019).
<https://doi.org:10.1038/s41467-019-10247-4>
- 3 Dyer, P. N. *et al.* Reconstitution of nucleosome core particles from recombinant histones and DNA. *Methods Enzymol* **375**, 23-44 (2004). [https://doi.org:10.1016/s0076-6879\(03\)75002-2](https://doi.org:10.1016/s0076-6879(03)75002-2)
- 4 Lowary, P. T. & Widom, J. New DNA sequence rules for high affinity binding to histone octamer and sequence-directed nucleosome positioning. *Journal of Molecular Biology* **276**, 19-42 (1998). <https://doi.org:DOI 10.1006/jmbi.1997.1494>
- 5 Luger, K., Rechsteiner, T. J. & Richmond, T. J. Preparation of nucleosome core particle from recombinant histones. *Methods Enzymol* **304**, 3-19 (1999).
[https://doi.org:10.1016/s0076-6879\(99\)04003-3](https://doi.org:10.1016/s0076-6879(99)04003-3)
- 6 Adams, M. K., Banks, C. A. S., Miah, S., Killer, M. & Washburn, M. P. Purification and enzymatic assay of class I histone deacetylase enzymes. *Method Enzymol* **626**, 23-40 (2019). <https://doi.org:10.1016/bs.mie.2019.07.014>
- 7 Zheng, S. Q. *et al.* MotionCor2: anisotropic correction of beam-induced motion for improved cryo-electron microscopy. *Nat Methods* **14**, 331-332 (2017).
<https://doi.org:10.1038/nmeth.4193>
- 8 Rohou, A. & Grigorieff, N. CTFFIND4: Fast and accurate defocus estimation from electron micrographs. *J Struct Biol* **192**, 216-221 (2015).
<https://doi.org:10.1016/j.jsb.2015.08.008>
- 9 Scheres, S. H. RELION: implementation of a Bayesian approach to cryo-EM structure determination. *Journal of structural biology* **180**, 519-530 (2012).
<https://doi.org:10.1016/j.jsb.2012.09.006>
- 10 Punjani, A., Rubinstein, J. L., Fleet, D. J. & Brubaker, M. A. cryoSPARC: algorithms for rapid unsupervised cryo-EM structure determination. *Nat Methods* **14**, 290-296 (2017).
<https://doi.org:10.1038/nmeth.4169>
- 11 Wang, H. B., Farnung, L., Dienemann, C. & Cramer, P. Structure of H3K36-methylated nucleosome-PWWP complex reveals multivalent cross-gyre binding. *Nat Struct Mol Biol* **27**, 8-+ (2020). <https://doi.org:10.1038/s41594-019-0345-4>
- 12 Jumper, J. *et al.* Highly accurate protein structure prediction with AlphaFold. *Nature* **596**, 583-+ (2021). <https://doi.org:10.1038/s41586-021-03819-2>
- 13 Varadi, M. *et al.* AlphaFold Protein Structure Database: massively expanding the structural coverage of protein-sequence space with high-accuracy models. *Nucleic Acids Research* **50**, D439-D444 (2022). <https://doi.org:10.1093/nar/gkab1061>

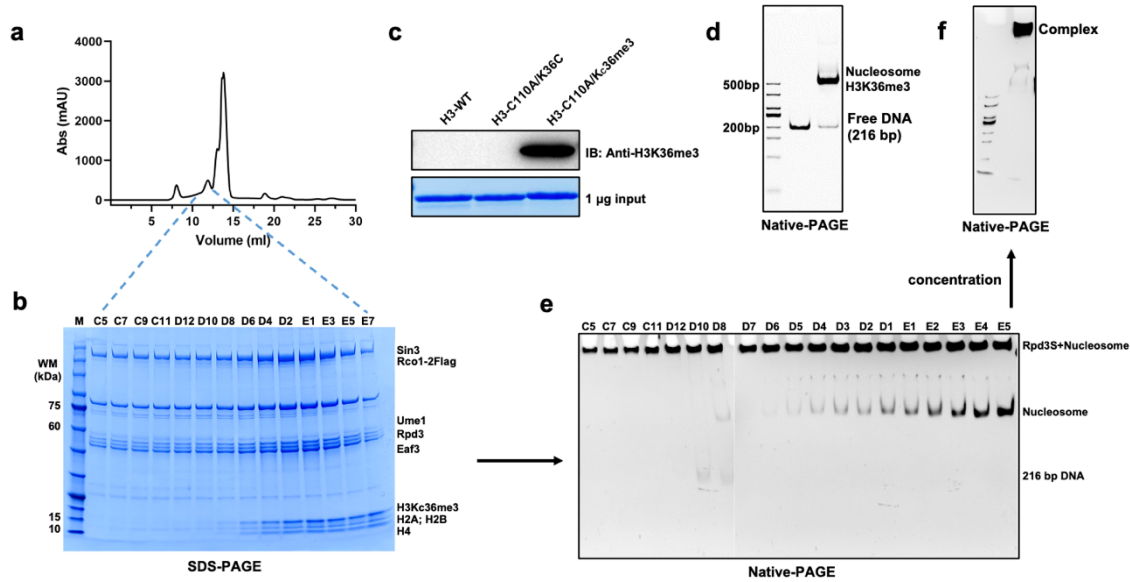
1 14 Pettersen, E. F. *et al.* UCSF Chimera--a visualization system for exploratory research and
2 analysis. *J Comput Chem* **25**, 1605-1612 (2004). <https://doi.org:10.1002/jcc.20084>
3 15 Emsley, P. & Cowtan, K. Coot: model-building tools for molecular graphics. *Acta*
4 *Crystallogr D Biol Crystallogr* **60**, 2126-2132 (2004).
5 <https://doi.org:10.1107/S0907444904019158>
6 16 Adams, P. D. *et al.* PHENIX: a comprehensive Python-based system for macromolecular
7 structure solution. *Acta Crystallogr D Biol Crystallogr* **66**, 213-221 (2010).
8 <https://doi.org:10.1107/S0907444909052925>
9 17 Goddard, T. D. *et al.* UCSF ChimeraX: Meeting modern challenges in visualization and
10 analysis. *Protein Sci* **27**, 14-25 (2018). <https://doi.org:10.1002/pro.3235>

11

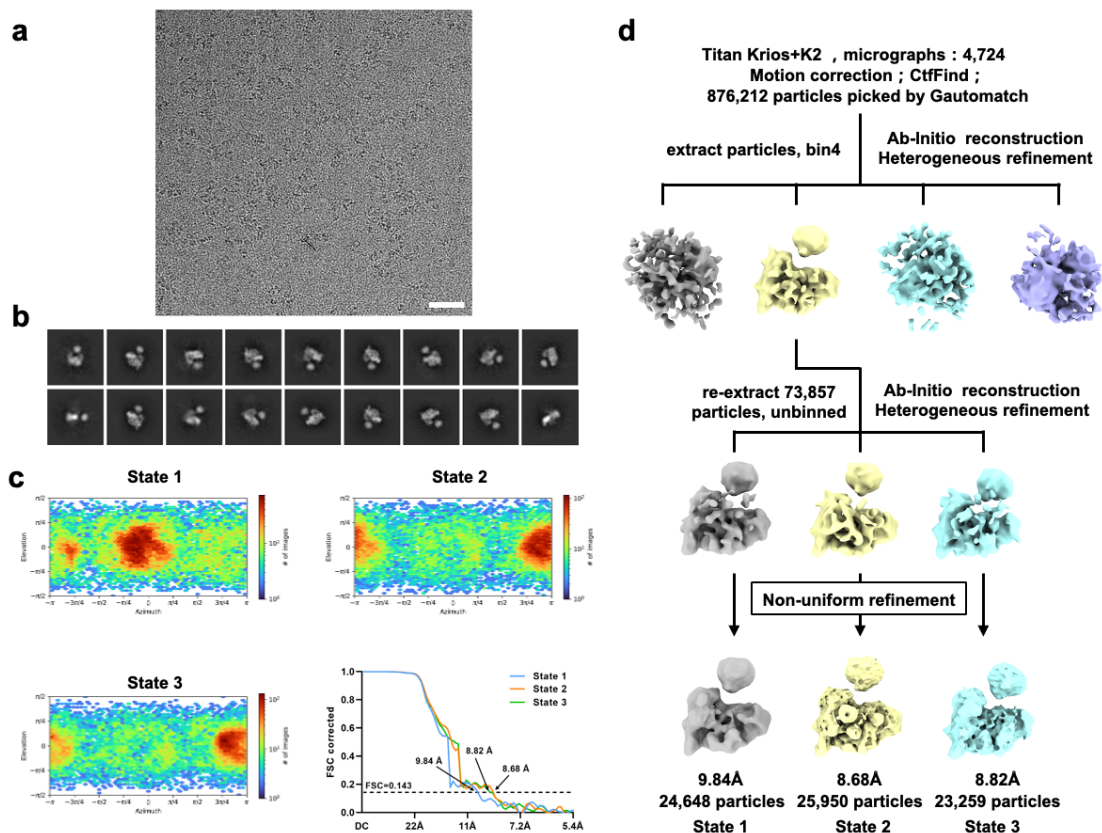
12



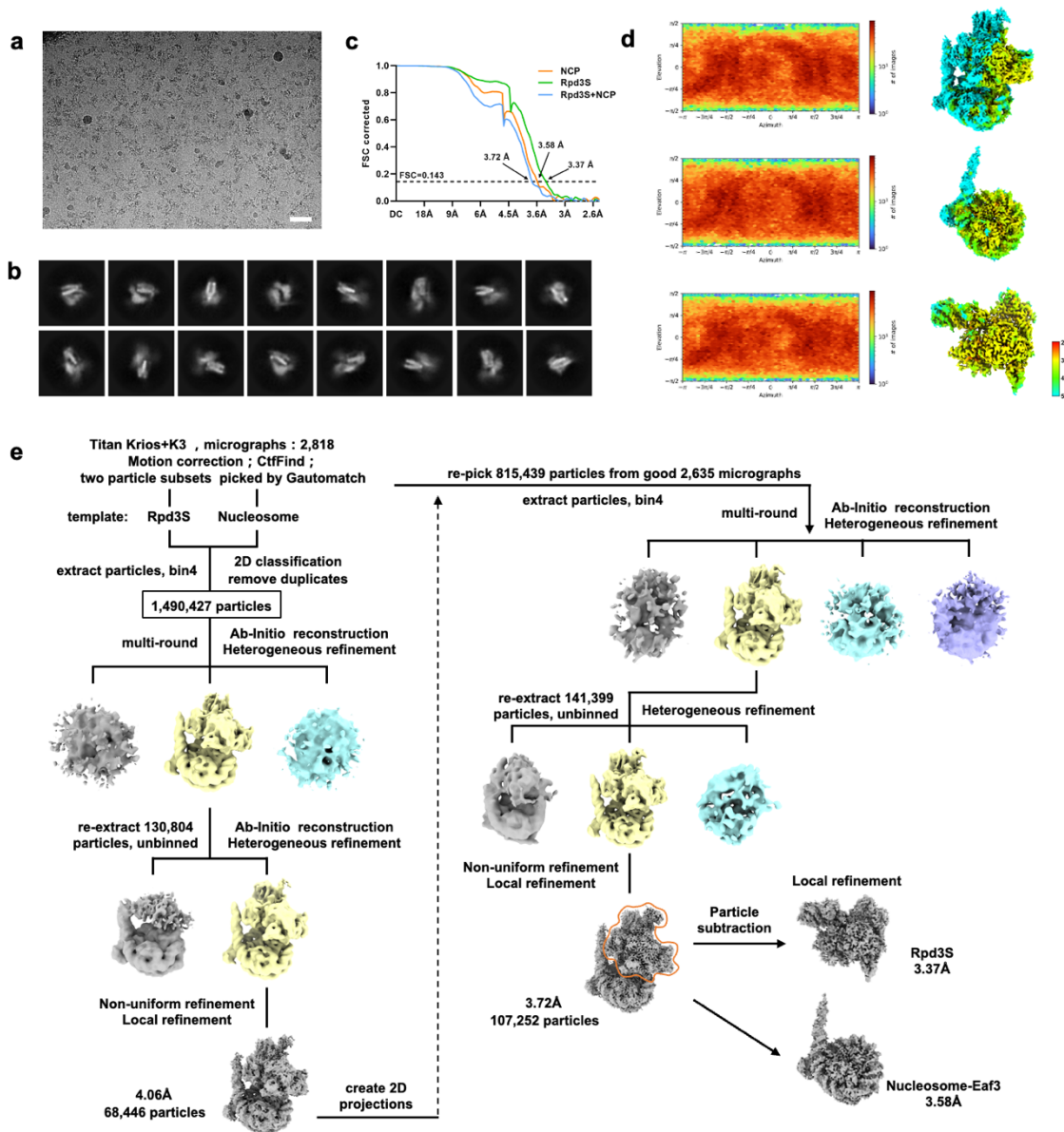
Extended Data Figure 1 | Purification and preliminary EM analysis of the Rpd3S. a, Size-exclusion chromatogram of the endogenously purified Rpd3S from *S. cerevisiae*, using a Superose 6 10/300 GL gel filtration column and monitoring absorption at 280 nm. **b,** SDS-PAGE analysis of the purified Rpd3S (the first peak). **c,** *In vitro* deacetylase activity of the purified Rpd3S complex. **d,** A typical electron micrograph showing the appearance of the negative stained Rpd3S sample. **e,** A typical 2D class average of Rpd3S preserved under negative stain.



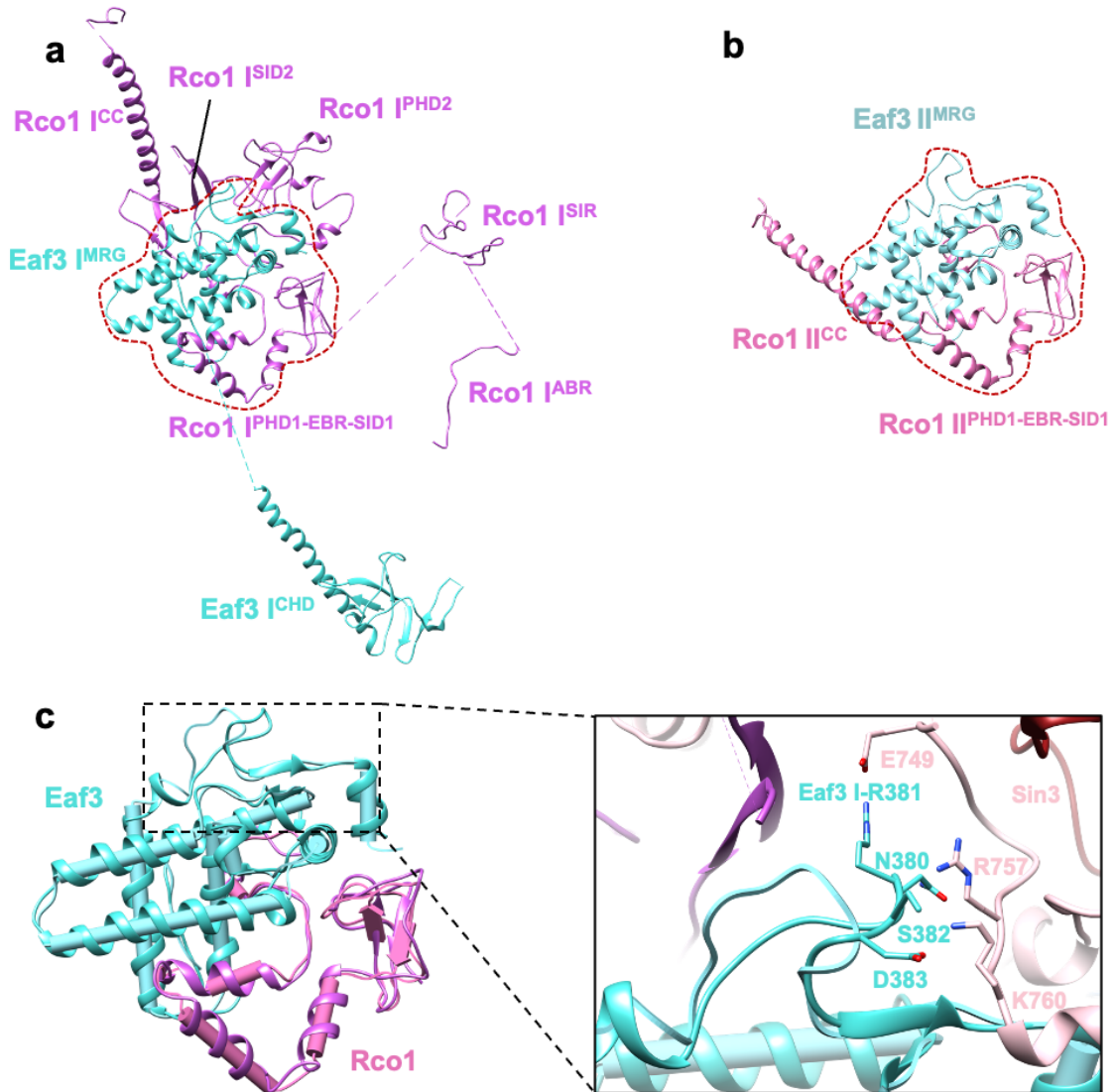
Extended Data Figure 2 | Rpd3S-nucleosome complex assembly. **a**, Purification of the Rpd3S-nucleosome complex Superose 6 10/300 GL column. **b**, SDS-PAGE analysis of the Rpd3S-nucleosome complex peak (~12 ml). **c**, The identification of the H3Kc36me3-modified H3 was performed by Western blotting. **d**, The reconstituted mononucleosome with 216 bp DNA was assessed by Native-PAGE. **e**, The Rpd3S-nucleosome complex fractions were assessed by Native-PAGE and the fractions from C5 to E5 were selected for cryo-EM analysis. **f**, The concentrated Rpd3S-nucleosome complex was assessed by Native-PAGE before cryo-EM grids preparation.



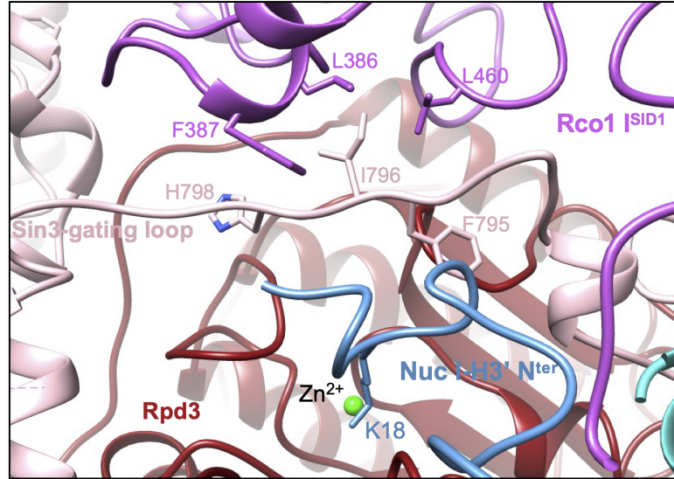
Extended Data Figure 3 | Cryo-EM data processing of *S. cerevisiae* Rpd3S. **a**, A typical micrograph of the Rpd3S preserved in vitrified ice. Scale bar, 50 nm. **b**, Typical 2D class averages obtained after reference-free alignment and classification of images of Rpd3S particles. **c**, Heat maps showing particle orientation distribution and Gold-standard FSC curves of the reconstructed Rpd3S three conformations: state 1 map 9.84 Å, state 2 map 8.86 Å and state 3 map 8.82 Å (FSC = 0.143). **d**, Flow chart of cryo-EM data processing.



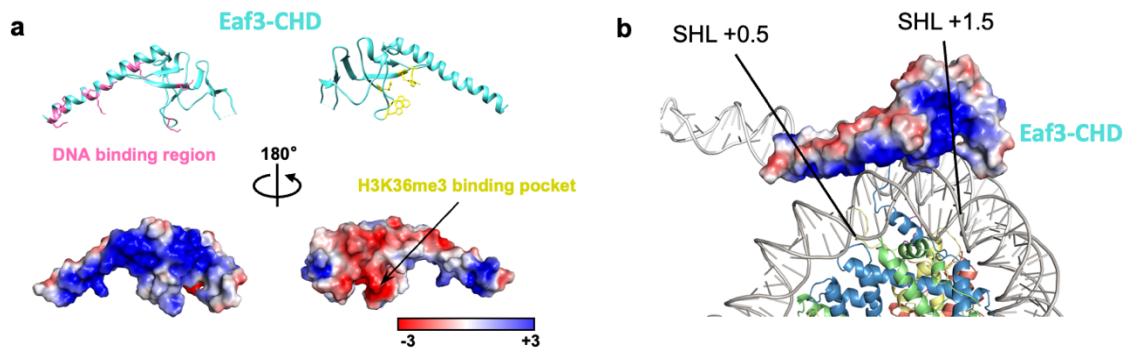
Extended Data Figure 4 | Rpd3S-nucleosome complex cryo-EM reconstruction. **a**, Representative micrograph of the dataset used to determine the Rpd3S-nucleosome complex structure. Scale bar, 50 nm. **b**, A typical reference-free 2D classes averages of Rpd3S-nucleosome. **c**, FSC curve for the cryo-EM density map according to the gold-standard criterion. The final resolution of Rpd3S-nucleosome is 3.72 Å, Rpd3S core 3.37 Å, and nucleosome-Eaf3 3.58 Å. **d**, Angular distributions of particles used in the final 3D reconstruction (left) and the local resolution of the corresponding cryo-EM map (right), Rpd3S-nucleosome (top), nucleosome-Eaf3 (middle), Rpd3S core (bottom). **e**, Image processing scheme. Particles were picked using different templates to achieve higher map resolution, also performed particle subtraction and local refinement.



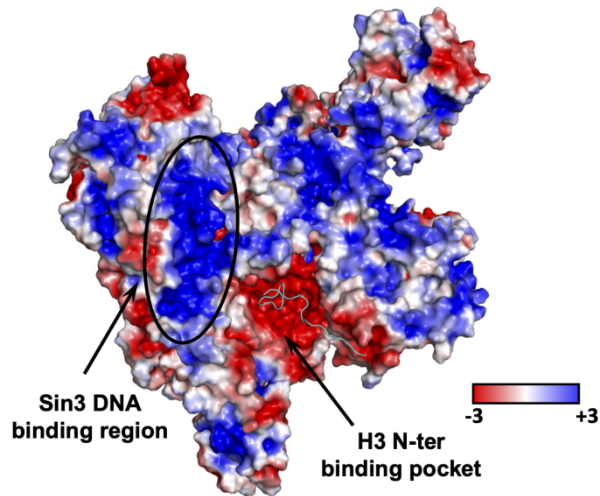
Extended Data Figure 5 | The comparison between Eaf3-Rco1 two copies in Rpd3S-nucleosome complex. a-b, Eaf3 MRG domain and Rco1 PHD-EBR-SID1 domain of copy 1 were highlighted by the red dotted line, the same view of Eaf3-Rco1 copy 2 shown in **b**. **c**, Eaf3-Rco1 two copies were merged (left) and the close-up view of the significant difference in the loop of Eaf3 (375-383 residues) shown (right).



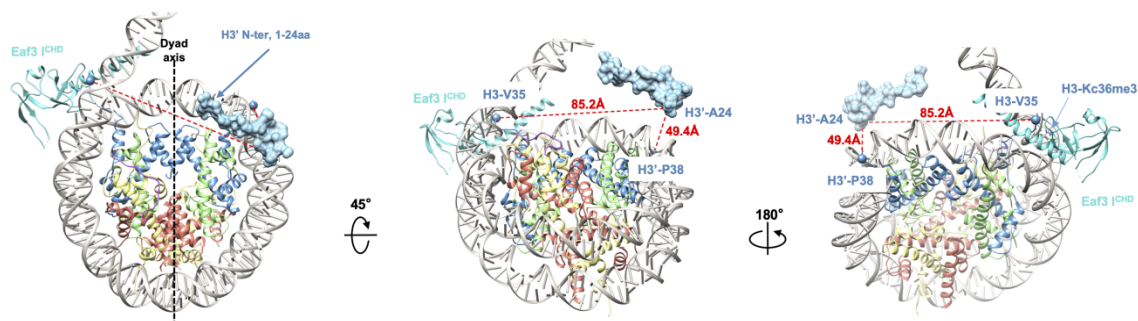
Extended Data Figure 6 | The close-up view of the histone H3 substrate catalytic site. The side chain of H3K18 deposited into the Rpd3 HDAC active core is shown, and the side chain of residues involved in the interface between Rco1-SID1 and Sin3-gating loop is denoted.



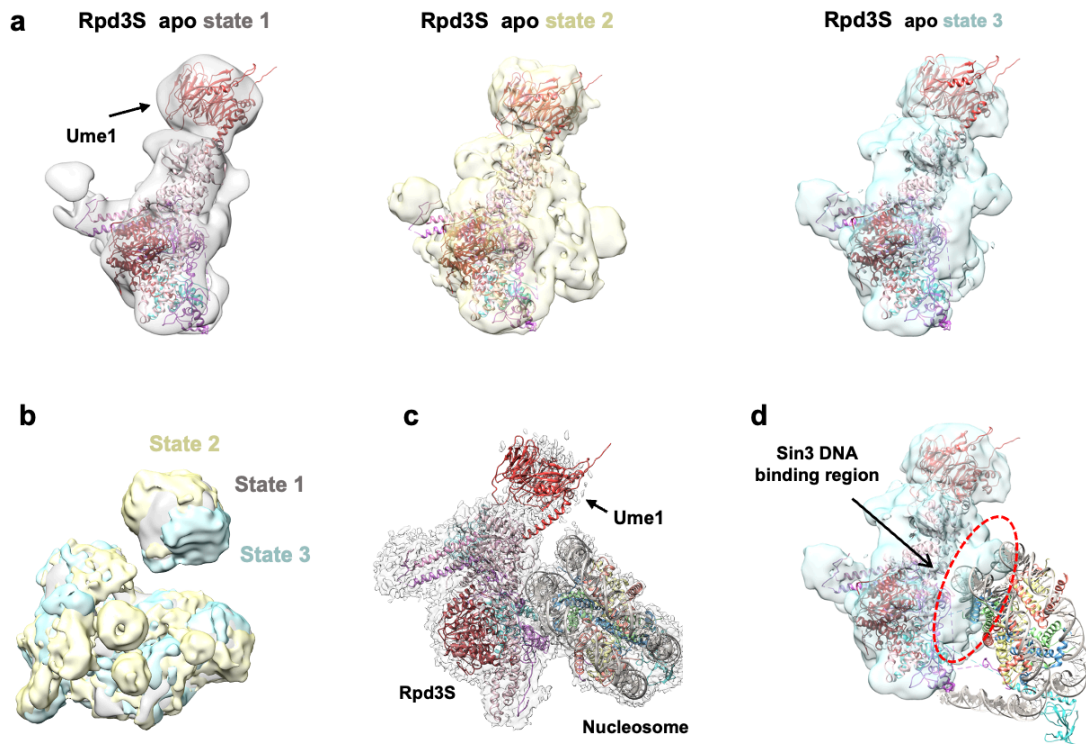
Extended Data Figure 7 | Binding of Eaf3 CHD domain to H3K36me3 and nucleosome DNA. **a**, Electrostatic surface of the Eaf3 CHD domain calculated using the APBS tool (bottom). The positively charged surface involved in DNA interaction and the residues are colored in pink (top left); the residues involved in H3K36me3 recognition are colored in yellow (top right). **b**, Details of DNA interactions. SHLs are denoted.



Extended Data Figure 8 | Electrostatic analysis of the Sin3 DNA binding region and the substrate binding pocket. Electrostatic surface of the Rpd3S core complex calculated using the APBS tool in a range of -3 kT e^{-1} to $+3 \text{ kT e}^{-1}$. The positively charged surface is consistent with the DNA binding region of Sin3, and the catalytic substrate H3 N-ter (shown in ribbon) deposited in the negatively charged pocket.



Extended Data Figure 9 | The histone H3 tail deposited in the catalytic pocket is different from the H3 bound by Eaf3. The histone H3 N-ter (1-24 residues) in catalytic site are shown as surface. The distances of the H3 A24 residue to the two H3 tails are shown in red with different views.



Extended Data Figure 10 | The potential location of Ume1 in Rpd3S holoenzyme. a, Ume1 structure from AlphaFold protein structure database is denoted and fitted into the Rpd3S apo states maps. **b,** The comparison between the Rpd3S apo states (shown in different colors). **c,** Ume1 fitted in the disordered region of Rpd3S-nucleosome complex. **d,** Sin3 DNA binding region is occupied by additional density (highlighted by the red dotted line) in Rpd3S apo state.

1 **Extended Data Table. Statistics of 3D reconstruction and model refinement**
2

	NCP-Eaf3 (PDB 8IHM) (EMDB- 35449)	Rpd3S core (PDB 8IHN) (EMDB- 35450)	Rpd3S-NCP (PDB 8IHT) (EMDB- 35455)	Rpd3S apo state 1 (EMDB- 35456)	Rpd3S apo state 2 (EMDB- 35457)	Rpd3S apo state 3 (EMDB- 35458)
Data collection and processing						
Microscope	Krios G3	Krios G3	Krios G3	Krios G3	Krios G3	Krios G3
Camera	K3	K3	K3	K2	K2	K2
Voltage (kV)	300	300	300	300	300	300
Magnification	81,000	81,000	81,000	18,000	18,000	18,000
Electron exposure (e ⁻ /Å ²)	53	53	53	59	59	59
Pixel size (Å)	1.07	1.07	1.07	1.35	1.35	1.35
Frames (no.)	32	32	32	36	36	36
Defocus range (μm)	1.8-2.8	1.8-2.8	1.8-2.8	2.5-3.5	2.5-3.5	2.5-3.5
Symmetry imposed	C1	C1	C1	C1	C1	C1
Micrographs (no.)	2,818	2,818	2,818	4,724	4,724	4,724
Initial particle images (no.)	815,439	815,439	815,439	876,212	876,212	876,212
Final particle images (no.)	107,252	107,252	107,252	24,648	25,950	23,259
Map resolution (Å)	3.58	3.37	3.72	9.84	8.68	8.82
FSC threshold	0.143	0.143	0.143	0.143	0.143	0.143
Model building						
Software	Coot	Coot	Coot			
Refinement						
Software	Phenix	Phenix	Phenix			
Model-map scores						
CC (mask)	0.83	0.82	0.82			
CC (box)	0.83	0.77	0.85			
CC (peaks)	0.76	0.71	0.76			
CC (volume)	0.82	0.81	0.81			
Validation						
R.m.s deviations						
Bonds length (Å)	0.010	0.005	0.009			
Bonds Angle (°)	0.837	0.725	0.904			
Ramachandran plot						
Favored (%)	95.37	92.39	91.17			
Allowed (%)	4.17	7.08	8.06			
Outlier (%)	0.46	0.53	0.77			